

NUMERICAL ANALYSIS AND SCIENTIFIC COMPUTING  
PREPRINT SERIA

**A  $C^0$  interior penalty discontinuous Galerkin  
method for fourth order total variation flow.  
I: Derivation of the method and numerical  
results**

C. BHANDARI      R. H. W. HOPPE      R. KUMAR

PREPRINT #64



DEPARTMENT OF MATHEMATICS  
UNIVERSITY OF HOUSTON

JANUARY 2019

# A $C^0$ INTERIOR PENALTY DISCONTINUOUS GALERKIN METHOD FOR FOURTH ORDER TOTAL VARIATION FLOW. I: DERIVATION OF THE METHOD AND NUMERICAL RESULTS.

C. BHANDARI<sup>1</sup>, R.H.W. HOPPE<sup>2</sup>, AND R. KUMAR<sup>3</sup>

ABSTRACT. We consider the numerical solution of a fourth order total variation flow problem representing surface relaxation below the roughening temperature. Based on a regularization and scaling of the nonlinear fourth order parabolic equation, we perform an implicit discretization in time and a  $C^0$  Interior Penalty Discontinuous Galerkin ( $C^0$ IPDG) discretization in space. The  $C^0$ IPDG approximation can be derived from a mixed formulation involving numerical flux functions where an appropriate choice of the flux functions allows to eliminate the discrete dual variable. The fully discrete problem can be interpreted as a parameter dependent nonlinear system with the discrete time as a parameter. It is solved by a predictor corrector continuation strategy featuring an adaptive choice of the time step sizes. A documentation of numerical results is provided illustrating the performance of the  $C^0$ IPDG method and the predictor corrector continuation strategy. The existence and uniqueness of a solution of the  $C^0$ IPDG method will be shown in the second part of this paper.

## 1. INTRODUCTION

Surface relaxation by surface diffusion is about the relaxation of a high symmetry crystalline surface on which a particular profile has been imprinted such that the typical length scale of the imposed profile is much larger than the lattice constant (dimension of unit cells in the crystal lattice). Therefore, surface relaxation is an important process in material sciences, in particular in the production of nanotechnology devices. The problem is to understand along which route the initial profile relaxes to a completely flat surface. One distinguishes between relaxation above and below the roughening temperature. Below the roughening temperature, the surface free energy has a cusp singularity. Several authors have suggested to model the dynamics by a total variation  $H^{-1}$  flow problem that can be formulated as a fourth order total variation flow (TVF) problem (cf., e.g., [8, 15, 22, 23, 28, 29, 30, 31]).

---

1991 *Mathematics Subject Classification.* 35K35,35K55,65M60.

*Key words and phrases.*  $C^0$  interior penalty discontinuous Galerkin method, fourth order total variation flow, surface relaxation.

<sup>1</sup> Department of Mathematics, University of Houston, USA.

<sup>2</sup> Department of Mathematics, University of Augsburg, Germany, and Department of Mathematics, University of Houston, USA. The work of the authors has been supported by the NSF grant DMS-1520886.

<sup>3</sup> Basque Center for Applied Mathematics, Bilbao, Spain.

Given a bounded domain  $\hat{\Omega} \subset \mathbb{R}^2$  with boundary  $\hat{\Gamma} = \partial\hat{\Omega}$ , the total variation- $H^{-1}$  (TV- $H^{-1}$ ) minimization of the energy functional

$$(1.1) \quad E(w) = \beta \int_{\hat{\Omega}} |\nabla w| \, dx, \quad \beta > 0,$$

leads to the following fourth order total variation flow (TVF) problem

$$(1.2a) \quad \frac{\partial w}{\partial \hat{t}} + \beta \Delta \nabla \cdot \frac{\nabla w}{|\nabla w|} = 0 \quad \text{in } \hat{Q} := \hat{\Omega} \times (0, \hat{T}),$$

$$(1.2b) \quad \mathbf{n}_{\hat{\Gamma}} \cdot \beta \frac{\nabla w}{|\nabla w|} = \mathbf{n}_{\hat{\Gamma}} \cdot \nabla \nabla \left( \nabla \cdot \frac{\nabla w}{|\nabla w|} \right) = 0 \quad \text{on } \hat{\Sigma} := \hat{\Gamma} \times (0, \hat{T}),$$

$$(1.2c) \quad w(\cdot, 0) = w^0 \quad \text{in } \hat{\Omega},$$

where  $\beta > 0$  is related to the mobility,  $\hat{T} > 0$  is the final time,  $\mathbf{n}_{\hat{\Gamma}}$  stands for the exterior unit normal at  $\hat{\Gamma}$ , and  $w^0 \in L^2(\hat{\Omega})$  is some given initial data. The fourth order equation (1.2a) has to be interpreted as follows: On  $H^{-1}(\hat{\Omega})$  we introduce an inner product according to

$$(w, z)_{-1, \hat{\Omega}} := (\nabla(-\Delta^{-1}w), \nabla(-\Delta^{-1}z))_{0, \hat{\Omega}},$$

where  $\Delta^{-1}$  stands for the inverse of the Laplacian. For  $E(w) = \beta \int_{\hat{\Omega}} |\nabla w| \, dx$ ,  $w \in H^{-1}(\hat{\Omega})$ , with  $D(E) = \{w \in H^{-1}(\hat{\Omega}) \mid E(w) < \infty\}$ , the subdifferential

$$\partial_{H^{-1}} E(w) = \{v \in H^{-1}(\hat{\Omega}) \mid (v, z - w)_{-1, \hat{\Omega}} \leq E(z) - E(w) \text{ for all } z \in H^{-1}(\hat{\Omega})\}$$

is given by (cf., e.g., [19])

$$\partial_{H^{-1}} E(w) = \{\Delta \nabla \cdot \boldsymbol{\xi} \mid \boldsymbol{\xi}(\hat{x}) \in \partial\Phi(\nabla w(\hat{x}))\},$$

where  $\Phi(|\boldsymbol{\eta}|)$  and  $\partial\Phi(|\boldsymbol{\eta}|)$  are given by

$$(1.3) \quad \Phi(\boldsymbol{\eta}) = \beta |\boldsymbol{\eta}|, \quad \partial\Phi(\boldsymbol{\eta}) = \begin{cases} \beta \boldsymbol{\eta} / |\boldsymbol{\eta}|, & \text{if } \boldsymbol{\eta} \neq \mathbf{0} \\ \{\boldsymbol{\tau} \in \mathbb{R}^2 \mid |\boldsymbol{\tau}| \leq \beta\}, & \text{if } \boldsymbol{\eta} = \mathbf{0} \end{cases}.$$

We thus obtain

$$-\frac{\partial w}{\partial \hat{t}} \in \partial E_{H^{-1}}(w).$$

Initial-boundary value problems for fourth order TVF problems have been considered mainly from an analytical point of view (cf., e.g., [13, 14, 19, 20, 21]).

Here, we consider the regularized TV- $H^{-1}$  energy functional

$$E_{reg}(w) = \beta \int_{\hat{\Omega}} (\delta^2 + |\nabla w|^2)^{1/2} \, dx, \quad w \in H^{-1}(\hat{\Omega}),$$

where  $\delta > 0$  is a regularization parameter. This leads to the regularized fourth order TVF problem

$$(1.4a) \quad \frac{\partial w}{\partial \hat{t}} + \beta \Delta \nabla \cdot ((\delta^2 + |\nabla w|^2)^{-1/2} \nabla w) = 0 \quad \text{in } \hat{Q},$$

$$(1.4b) \quad \mathbf{n}_{\hat{\Gamma}} \cdot \beta (\delta^2 + |\nabla w|^2)^{-1/2} \nabla w = 0 \quad \text{on } \hat{\Sigma},$$

$$\mathbf{n}_{\hat{\Gamma}} \cdot \beta \nabla \left( \nabla \cdot ((\delta^2 + |\nabla w|^2)^{-1/2} \nabla w) \right) = 0 \quad \text{on } \hat{\Sigma},$$

$$(1.4c) \quad w(\cdot, 0) = w^0 \quad \text{in } \hat{\Omega}.$$

We further consider a scaling in both the time variable and the spatial variables according to

$$(1.5) \quad t = \delta \hat{t}, \quad x_i = \delta \hat{x}_i, \quad 1 \leq i \leq 2.$$

Setting  $T := \delta \hat{T}$ ,  $\Omega := \delta \hat{\Omega}$ ,  $\Gamma := \partial\Omega$ ,  $Q := \Omega \times (0, T)$ ,  $\Sigma := \Gamma \times (0, T)$ , and  $u^0(x) = w^0(\delta^{-1}x)$ , as well as

$$(1.6) \quad \omega(\nabla u) := 1 + |\nabla u|^2,$$

the scaled regularized fourth order TVF problem reads as follows

$$(1.7a) \quad \frac{\partial u}{\partial t} + \beta \delta^2 \Delta \nabla \cdot (\omega(\nabla u)^{-1/2} \nabla u) = 0 \quad \text{in } Q,$$

$$(1.7b) \quad \mathbf{n}_\Gamma \cdot \beta \delta^2 (\omega(\nabla u)^{-1/2} \nabla u) = \mathbf{n}_\Gamma \cdot \beta \delta^2 \nabla \left( \nabla \cdot (\omega(\nabla u)^{-1/2} \nabla u) \right) = 0 \quad \text{on } \Sigma,$$

$$(1.7c) \quad u(\cdot, 0) = u^0 \quad \text{in } \Omega.$$

The numerical solution of the regularized fourth order TVF problem with periodic boundary conditions has been considered in [22] based on a mixed formulation of the implicitly in time discretized problem. At each time-step, this amounts to the solution of two second order elliptic PDEs by standard Lagrangian finite elements with respect to a triangulation of the computational domain  $\Omega$ . On the other hand, Interior Penalty Discontinuous Galerkin (IPDG) methods for fourth order elliptic boundary value problems, fourth order and higher order polyharmonic parabolic initial-boundary value problems have been studied in [2, 3, 4, 5, 6, 7, 11, 12, 17, 18, 25, 26, 32, 36]. The advantage of the C<sup>0</sup>IPDG approach is that it directly applies to the fourth order problem and thus only requires the numerical solution of one equation by using the same Lagrangian finite elements as in the mixed method.

**Remark 1.1.** *We note that another example for a TV-H<sup>-1</sup> minimization problem is the minimization of the energy functional*

$$E(w, \hat{g}) = \int_{\hat{\Omega}} |\nabla w| \, dx + \frac{\lambda}{2} \|w - \hat{g}\|_{H^{-1}(\hat{\Omega})}^2$$

which occurs in image recovery where  $w$  represents a true image,  $\hat{g}$  describes a blurred and/or noisy image, and  $\lambda > 0$  is a fidelity parameter (cf. [24, 27, 34, 35]). The associated fourth order total variation flow (TVF) problem is given by the initial-boundary value problem

$$(1.8a) \quad \frac{\partial w}{\partial \hat{t}} + \lambda^{-1} \Delta \nabla \cdot \frac{\nabla w}{|\nabla w|} + w - \hat{g} = 0 \quad \text{in } \hat{Q},$$

$$(1.8b) \quad \mathbf{n}_{\hat{\Gamma}} \cdot \frac{\nabla w}{|\nabla w|} = \mathbf{n}_{\hat{\Gamma}} \cdot \nabla \left( \nabla \cdot \frac{\nabla w}{|\nabla w|} \right) = 0 \quad \text{on } \hat{\Sigma},$$

$$(1.8c) \quad w(\cdot, 0) = w^0 \quad \text{in } \hat{\Omega}.$$

The paper is organized as follows: In section 2, we will perform a discretization in time of the regularized and scaled fourth order TVF problem and consider a reformulation in terms of the matrix of second order partial derivatives of the unknown. Section 3 is devoted to the derivation of the C<sup>0</sup>IPDG approximation based on an appropriate choice of numerical flux functions. In section 4, we will show that the fully discrete system can be written as a parameter dependent nonlinear system with the discrete time as a parameter. Since the choice of the time steps is crucial

for the convergence of Newton's method, we suggest a predictor corrector continuation strategy with constant continuation as a predictor and Newton's method as a corrector featuring an adaptive choice of the time step sizes. This avoids a breakdown of Newton's method due to convergence failure because of too large time steps. Finally, in section 5 we present numerical results illustrating the performance of the C<sup>0</sup>IPDG method and the predictor corrector continuation strategy.

Throughout the paper we will use the following notations and basic results. For vectors  $\mathbf{x} = (x_1, \dots, x_n)^T, \mathbf{y} = (y_1, \dots, y_n)^T \in \mathbb{R}^n$  and for matrices  $\underline{\mathbf{A}} = (a_{ij})_{i,j=1}^n, \underline{\mathbf{B}} = (b_{ij})_{i,j=1}^n \in \mathbb{R}^{n \times n}$  we denote by  $\mathbf{x} \cdot \mathbf{y}$  and  $\underline{\mathbf{A}} : \underline{\mathbf{B}}$  the Euclidean inner product  $\mathbf{x} \cdot \mathbf{y} = \sum_{i=1}^n x_i y_i$  and the Frobenius inner product  $\underline{\mathbf{A}} : \underline{\mathbf{B}} = \sum_{i,j=1}^n a_{ij} b_{ij}$ . In particular,  $|\mathbf{x}| := (\mathbf{x} \cdot \mathbf{x})^{1/2}$  and  $|\underline{\mathbf{A}}| := (\underline{\mathbf{A}} : \underline{\mathbf{A}})^{1/2}$  refer to the Euclidean norm and the Frobenius norm, respectively.

We will further use standard notation from Lebesgue and Sobolev space theory (cf., e.g., [33]). In particular, for a bounded domain  $D \subset \mathbb{R}^d, d \in \mathbb{N}$ , we refer to  $L^2(D)$  as the Hilbert space of square integrable functions on  $D$  with inner product  $(\cdot, \cdot)_{0,D}$  and norm  $\|\cdot\|_{0,D}$ . Moreover, we denote by  $H^m(D), m \in \mathbb{N}$ , the Sobolev space with inner product  $(\cdot, \cdot)_{m,D}$  and norm  $\|\cdot\|_{m,D}$ .

## 2. IMPLICIT TIME-DISCRETIZATION

For the numerical solution of the regularized fourth order TVF problem (1.7) we perform a discretization in time with respect to a partition of the time interval  $[0, T]$  into subintervals  $[t_{m-1}, t_m]$  of length  $\tau_m := t_m - t_{m-1}$ . Denoting by  $u^m$  some approximation of  $u$  at time  $t_m$ , for  $1 \leq m \leq M$  we have to solve the problems

$$(2.1a) \quad u^m - u^{m-1} + \tau_m \beta \delta^2 \Delta \nabla \cdot (\omega (\nabla u^m)^{-1/2} \nabla u^m) = 0 \text{ in } \Omega,$$

$$(2.1b)$$

$$\mathbf{n}_\Gamma \cdot \beta \delta^2 (\omega (\nabla u^m)^{-1/2} \nabla u^m) = \mathbf{n}_\Gamma \cdot \beta \delta^2 \nabla \left( \nabla \cdot (\omega (\nabla u^m)^{-1/2} \nabla u^m) \right) = 0 \text{ on } \Gamma.$$

Introducing the objective functional

$$(2.2) \quad J(v) := \frac{1}{2} \|v - u^{m-1}\|_{-1,\Omega}^2 + \tau_m \beta \delta^2 \int_{\Omega} (1 + |\nabla v|^2)^{1/2} dx,$$

it is easy to see that (2.1) is related to the necessary and sufficient optimality condition for the minimization problem

$$(2.3) \quad J(u^m) = \inf_{v \in H^{-1}(\Omega)} J(v),$$

which has a unique solution, since the objective functional  $J$  is strictly convex, coercive, and lower semicontinuous.

The fourth order equation (2.1a) can be reformulated in terms of the  $2 \times 2$  matrix

$$D^2 u^m = \begin{pmatrix} \frac{\partial^2 u^m}{\partial x_1^2} & \frac{\partial^2 u^m}{\partial x_1 \partial x_2} \\ \frac{\partial^2 u^m}{\partial x_1 \partial x_2} & \frac{\partial^2 u^m}{\partial x_2^2} \end{pmatrix}.$$

of second partial derivatives of  $u^m$ . We note that the divergence of a matrix-valued function  $\underline{\mathbf{q}} = (q_{ij})_{i,j=1}^2$  with row vectors  $\underline{\mathbf{q}}^{(i)} = (q_{i1}, q_{i2})^T, 1 \leq i \leq 2$ , is defined by

means of

$$(2.4) \quad \nabla \cdot \underline{\mathbf{q}} := (\nabla \cdot \underline{\mathbf{q}}^{(1)}, \nabla \cdot \underline{\mathbf{q}}^{(2)})^T.$$

**Theorem 2.1.** *The fourth order equation (2.1a) is equivalent to*

$$(2.5) \quad u^m - u^{m-1} + \tau_m \beta \delta^2 \nabla \cdot \nabla \cdot (\omega(\nabla u^m)^{-3/2} \underline{\mathbf{M}}(u^m) D^2 u^m) = 0,$$

where  $\underline{\mathbf{M}}(v)$  stands for the matrix-valued function

$$(2.6) \quad \underline{\mathbf{M}}(v) := \begin{pmatrix} 1 + \left(\frac{\partial v}{\partial x_2}\right)^2 & -\frac{\partial v}{\partial x_1} \frac{\partial v}{\partial x_2} \\ -\frac{\partial v}{\partial x_1} \frac{\partial v}{\partial x_2} & 1 + \left(\frac{\partial v}{\partial x_1}\right)^2 \end{pmatrix}.$$

*Proof.* We reformulate the second term on the left-hand side of (2.1a) according to

$$(2.7) \quad \begin{aligned} \Delta \nabla \cdot (\omega(\nabla u^m)^{-1/2} \nabla u^m) &= \nabla \cdot \nabla \left( \nabla \cdot (\omega(\nabla u^m)^{-1/2} \nabla u^m) \right) = \\ &= \nabla \cdot \nabla \cdot \nabla (\omega(\nabla u^m)^{-1/2} \nabla u^m). \end{aligned}$$

Obviously, we have

$$(2.8) \quad \nabla (\omega(\nabla u^m)^{-1/2} \nabla u^m) = \begin{pmatrix} \frac{\partial}{\partial x_1} \\ \frac{\partial}{\partial x_2} \end{pmatrix} \left( \omega(\nabla u^m)^{-1/2} \begin{pmatrix} \frac{\partial u^m}{\partial x_1} \\ \frac{\partial u^m}{\partial x_2} \end{pmatrix} \right).$$

In particular,

$$(2.9) \quad \begin{aligned} &\frac{\partial}{\partial x_1} \left( \omega(\nabla u^m)^{-1/2} \begin{pmatrix} \frac{\partial u^m}{\partial x_1} \\ \frac{\partial u^m}{\partial x_2} \end{pmatrix} \right) = \\ &= -\omega(\nabla u^m)^{-3/2} \left( \frac{\partial u^m}{\partial x_1} \frac{\partial^2 u^m}{\partial x_1^2} + \frac{\partial u^m}{\partial x_2} \frac{\partial^2 u^m}{\partial x_1 \partial x_2} \right) \begin{pmatrix} \frac{\partial u^m}{\partial x_1} \\ \frac{\partial u^m}{\partial x_2} \end{pmatrix} + \\ &\omega(\nabla u^m)^{-1/2} \begin{pmatrix} \frac{\partial^2 u^m}{\partial x_1^2} \\ \frac{\partial^2 u^m}{\partial x_1 \partial x_2} \end{pmatrix} = \\ &\omega(\nabla u^m)^{-3/2} \begin{pmatrix} \left(1 + \left(\frac{\partial u^m}{\partial x_2}\right)^2\right) \frac{\partial^2 u^m}{\partial x_1^2} - \frac{\partial u^m}{\partial x_1} \frac{\partial u^m}{\partial x_2} \frac{\partial^2 u^m}{\partial x_1 \partial x_2} \\ \left(1 + \left(\frac{\partial u^m}{\partial x_1}\right)^2\right) \frac{\partial^2 u^m}{\partial x_1 \partial x_2} - \frac{\partial u^m}{\partial x_1} \frac{\partial u^m}{\partial x_2} \frac{\partial^2 u^m}{\partial x_1^2} \end{pmatrix}, \end{aligned}$$

and

$$\begin{aligned}
(2.10) \quad & \frac{\partial}{\partial x_2} \left( \omega(\nabla u^m)^{-1/2} \begin{pmatrix} \frac{\partial u^m}{\partial x_1} \\ \frac{\partial u^m}{\partial x_2} \end{pmatrix} \right) = \\
& -\omega(\nabla u^m)^{-3/2} \left( \frac{\partial u^m}{\partial x_1} \frac{\partial^2 u^m}{\partial x_1 \partial x_2} + \frac{\partial u^m}{\partial x_2} \frac{\partial^2 u^m}{\partial x_2^2} \right) \begin{pmatrix} \frac{\partial u^m}{\partial x_1} \\ \frac{\partial u^m}{\partial x_2} \end{pmatrix} + \\
& \omega(\nabla u^m)^{-1/2} \begin{pmatrix} \frac{\partial^2 u^m}{\partial x_1 \partial x_2} \\ \frac{\partial^2 u^m}{\partial x_2^2} \end{pmatrix} = \\
& \omega(\nabla u^m)^{-3/2} \begin{pmatrix} \left( 1 + \left( \frac{\partial u^m}{\partial x_2} \right)^2 \frac{\partial^2 u^m}{\partial x_1 \partial x_2} - \frac{\partial u^m}{\partial x_1} \frac{\partial u^m}{\partial x_2} \frac{\partial^2 u^m}{\partial x_1^2} \right) \\ \left( 1 + \left( \frac{\partial u^m}{\partial x_1} \right)^2 \frac{\partial^2 u^m}{\partial x_2^2} - \frac{\partial u^m}{\partial x_1} \frac{\partial u^m}{\partial x_2} \frac{\partial^2 u^m}{\partial x_1 \partial x_2} \right) \end{pmatrix}.
\end{aligned}$$

Using (2.9) and (2.10) in (2.8), it follows that

$$\begin{aligned}
(2.11) \quad & \nabla(\omega(\nabla u^m)^{-1/2} \nabla u^m) = \\
& \omega(\nabla u^m)^{-3/2} \begin{pmatrix} 1 + \left( \frac{\partial u^m}{\partial x_2} \right)^2 & -\frac{\partial u^m}{\partial x_1} \frac{\partial u^m}{\partial x_2} \\ -\frac{\partial u^m}{\partial x_1} \frac{\partial u^m}{\partial x_2} & 1 + \left( \frac{\partial u^m}{\partial x_1} \right)^2 \end{pmatrix} D^2 u^m,
\end{aligned}$$

which can be written as

$$(2.12) \quad \nabla(\omega(\nabla u^m)^{-1/2} \nabla u^m) = \omega(\nabla u^m)^{-3/2} \underline{\underline{\mathbf{M}}}(u^m) D^2 u^m.$$

□

**Remark 2.1.** The matrix  $\underline{\underline{\mathbf{M}}}(v)$  is symmetric positive definite with the eigenvalues

$$(2.13) \quad \lambda_{\min}(\underline{\underline{\mathbf{M}}}(v)) = 1, \quad \lambda_{\max}(\underline{\underline{\mathbf{M}}}(v)) = 1 + |\nabla v|^2.$$

For notational convenience we set

$$(2.14) \quad \underline{\underline{\mathbf{A}}}_1(v) := \omega(\nabla v)^{-3/2} \underline{\underline{\mathbf{M}}}(v).$$

The weak formulation of (2.5) reads: Find

$$u^m \in V := \{v \in H^2(\Omega) \mid \mathbf{n}_\Gamma \cdot \beta \delta^2 \omega(\nabla v)^{-1/2} \nabla v = 0 \text{ on } \Gamma\}$$

such that for all  $v \in V$  it holds

$$(2.15) \quad (u^m - u^{m-1}, v)_{0,\Omega} + \tau_m \beta \delta^2 \int_{\Omega} \left( \underline{\underline{\mathbf{A}}}_1(u^m) D^2 u^m \right) : D^2 v \, dx = 0.$$

Finally, we provide a mixed formulation of (2.5), because the derivation of the C<sup>0</sup>IPDG method will be based on the discrete analogue of that mixed formulation. Introducing the matrix-valued function

$$(2.16) \quad \underline{\underline{\mathbf{p}}}^m := \omega(\nabla u^m)^{-1/4} D^2 u^m,$$

and the matrix

$$(2.17) \quad \underline{\mathbf{A}}_2(v) := \omega(\nabla v)^{-5/4} \underline{\mathbf{M}}(v).$$

the mixed formulation of (2.1a),(2.1b) reads as follows

$$(2.18a) \quad \underline{\mathbf{p}}^m - \omega(\nabla u^m)^{-1/4} D^2 u^m = 0 \text{ in } \Omega,$$

$$(2.18b) \quad u^m - u^{m-1} + \tau_m \beta \delta^2 \nabla \cdot \nabla \cdot \underline{\mathbf{A}}_2(u^m) \underline{\mathbf{p}}(u^m) = 0 \text{ in } \Omega,$$

$$(2.18c) \quad \mathbf{n}_\Gamma \cdot \beta \delta^2 \omega(\nabla u^m)^{-1/2} \nabla u^m = 0 \text{ on } \Gamma,$$

$$(2.18d) \quad \mathbf{n}_\Gamma \cdot \beta \delta^2 \nabla \cdot \underline{\mathbf{A}}_2(u^m) \underline{\mathbf{p}}^m = 0 \text{ on } \Gamma.$$

### 3. C<sup>0</sup> INTERIOR PENALTY DISCONTINUOUS GALERKIN APPROXIMATION

Let  $\mathcal{T}_h$  be a geometrically conforming, uniform simplicial triangulation of  $\Omega$ . We denote by  $\mathcal{E}_h(\Omega)$  and  $\mathcal{E}_h(\Gamma)$  the set of edges of  $\mathcal{T}_h$  in the interior of  $\Omega$  and on the boundary  $\Gamma$ , respectively, and set  $\mathcal{E}_h := \mathcal{E}_h(\Omega) \cup \mathcal{E}_h(\Gamma)$ . For  $K \in \mathcal{T}_h$  and  $E \in \mathcal{E}_h$  we denote by  $h_K$  and  $h_E$  the diameter of  $K$  and the length of  $E$ , and we set  $h := \max(h_K \mid K \in \mathcal{T}_h)$ . Due to the assumptions on  $\mathcal{T}_h$  there exist constants  $0 < c_R \leq C_R$ ,  $0 < c_Q \leq C_Q$ , and  $0 < c_S \leq C_S$  such that for all  $K \in \mathcal{T}_h$  it holds

$$(3.1a) \quad c_R h_K \leq h_E \leq C_R h_K, \quad E \in \mathcal{E}_h(\partial K),$$

$$(3.1b) \quad c_Q h \leq h_K \leq C_Q h,$$

$$(3.1c) \quad c_S h_K^2 \leq \text{meas}(K) \leq C_S h_K^2.$$

For two quantities  $A$  and  $B$  we write  $A \lesssim B$ , if there exists a constant  $C > 0$  independent of  $h$  such that  $A \leq CB$ .

Denoting by  $P_k(T)$ ,  $k \in \mathbb{N}$ , the linear space of polynomials of degree  $\leq k$  on  $T$ , for  $k \in \mathbb{N}$  we define

$$(3.2) \quad V_h := \{v_h \in C^0(\bar{\Omega}) \mid v_h|_T \in P_k(T), T \in \mathcal{T}_h\}$$

and note that  $V_h \subset H^1(\Omega)$ , but  $V_h \not\subset H^2(\Omega)$ . Further, we introduce

$$(3.3) \quad \underline{\mathbf{M}}_h := \{\underline{\mathbf{q}}_h \in L^2(\Omega)^{2 \times 2} \mid \underline{\mathbf{q}}_h|_K \in P_k(K)^{2 \times 2}, K \in \mathcal{T}_h\}$$

as the space of element-wise polynomial moment tensors.

For interior edges  $E \in \mathcal{E}_h(\Omega)$  such that  $E = K_+ \cap K_-$ ,  $K_\pm \in \mathcal{T}_h$  and boundary edges on  $\Gamma$  we introduce the average and jump of  $\nabla v_h$  according to

$$(3.4a) \quad \{\nabla v_h\}_E := \begin{cases} \frac{1}{2} \left( \nabla v_h|_{E \cap K_+} + \nabla v_h|_{E \cap K_-} \right), & E \in \mathcal{E}_h(\Omega) \\ \nabla v_h|_E, & E \in \mathcal{E}_h(\Gamma) \end{cases},$$

$$(3.4b) \quad [\nabla v_h]_E := \begin{cases} \nabla v_h|_{E \cap K_+} - \nabla v_h|_{E \cap K_-}, & E \in \mathcal{E}_h(\Omega) \\ \nabla v_h|_E, & E \in \mathcal{E}_h(\Gamma) \end{cases}.$$

The average  $\{\Delta v_h\}_E$  and jump  $[\Delta v_h]_E$  are defined analogously. We further denote by  $\mathbf{n}_E$  the unit normal vector on  $E$  pointing in the direction from  $K_+$  to  $K_-$ .

In order to motivate the C<sup>0</sup>IPDG approximation we will follow the approach taken in [1] for second order elliptic boundary value problems. For  $\underline{\mathbf{p}}_h^m \in \underline{\mathbf{M}}_h$  and  $u_h^m \in V_h$

we consider (2.18a),(2.18b) elementwise and (2.18c),(2.18d) edgewise, i.e.,

$$(3.5a) \quad \underline{\underline{\mathbf{p}}}_h^m - \omega(\nabla u_h^m)^{-1/4} D^2 u_h^m = 0 \quad \text{in } K \in \mathcal{T}_h,$$

$$(3.5b) \quad u_h^m - u_h^{m-1} + \tau_m \beta \delta^2 \nabla \cdot \nabla \cdot \underline{\underline{\mathbf{A}}}_2(u_h^m) \underline{\underline{\mathbf{p}}}_h^m = 0 \quad \text{in } K \in \mathcal{T}_h,$$

$$(3.5c) \quad \mathbf{n}_E \cdot \beta \delta^2 \omega(\nabla u_h^m)^{-1/4} \nabla u_h^m = 0 \quad \text{on } E \in \mathcal{E}_h(\Gamma),$$

$$(3.5d) \quad \mathbf{n}_E \cdot \beta \delta^2 \nabla \cdot \underline{\underline{\mathbf{A}}}_2(u_h^m) \underline{\underline{\mathbf{p}}}_h^m = 0 \quad \text{on } E \in \mathcal{E}_h(\Gamma),$$

with  $u_h^0 = Q_h u^0$ , where  $Q_h : L^2(\Omega) \rightarrow V_h$  denotes the  $L^2$  projection onto  $V_h$ . We multiply (3.5a) by  $\underline{\underline{\mathbf{q}}}_h \in \underline{\underline{\mathbf{M}}}_h$  and integrate over  $K$ :

$$(3.6) \quad \int_K \underline{\underline{\mathbf{p}}}_h^m : \underline{\underline{\mathbf{q}}}_h \, dx = \int_K (\omega(\nabla u_h^m)^{-1/4} D^2 u_h^m) : \underline{\underline{\mathbf{q}}}_h \, dx.$$

In view of (2.11) Green's formula yields

$$(3.7) \quad \begin{aligned} \int_K (\omega(\nabla u_h^m)^{-1/4} D^2 u_h^m) : \underline{\underline{\mathbf{q}}}_h \, dx &= \int_K D^2 u_h^m : (\omega(\nabla u_h^m)^{-1/4} \underline{\underline{\mathbf{q}}}_h) \, dx = \\ &= - \int_K \nabla u_h^m \cdot \nabla \cdot (\omega(\nabla u_h^m)^{-1/4} \underline{\underline{\mathbf{q}}}_h) \, dx + \int_{\partial K} \omega(\nabla u_h^m)^{-1/4} \nabla u_h^m \cdot \underline{\underline{\mathbf{q}}}_h \mathbf{n}_{\partial K} \, ds. \end{aligned}$$

On the other hand, we multiply (3.5b) by  $v_h \in V_h$  and integrate over  $K$ :

$$(3.8) \quad \int_K (u_h^m - u_h^{m-1}) v_h \, dx + \tau_m \beta \delta^2 \int_K \nabla \cdot \nabla \cdot \underline{\underline{\mathbf{A}}}_2(u_h^m) \underline{\underline{\mathbf{p}}}_h^m v_h \, dx = 0.$$

Applying Green's formula twice, we obtain

$$(3.9) \quad \begin{aligned} \int_K \nabla \cdot \nabla \cdot \underline{\underline{\mathbf{A}}}_2(u_h^m) \underline{\underline{\mathbf{p}}}_h^m v_h \, dx &= - \int_K \nabla \cdot \underline{\underline{\mathbf{A}}}_2(u_h^m) \underline{\underline{\mathbf{p}}}_h^m \cdot \nabla v_h \, dx + \\ &\int_{\partial K} \mathbf{n}_{\partial K} \cdot \nabla \cdot \underline{\underline{\mathbf{A}}}_2(u_h^m) \underline{\underline{\mathbf{p}}}_h^m v_h \, ds = \int_K \underline{\underline{\mathbf{p}}}_h^m : \underline{\underline{\mathbf{A}}}_2(u_h^m) D^2 v_h \, dx - \\ &\int_{\partial K} \underline{\underline{\mathbf{A}}}_2(u_h^m) \underline{\underline{\mathbf{p}}}_h^m \mathbf{n}_{\partial K} \cdot \nabla v_h \, ds + \int_{\partial K} \mathbf{n}_{\partial K} \cdot \nabla \cdot \underline{\underline{\mathbf{A}}}_2(u_h^m) \underline{\underline{\mathbf{p}}}_h^m v_h \, ds. \end{aligned}$$

Summing over all  $K \in \mathcal{T}_h$  in (3.7) and (3.9), we obtain the weak formulation of the mixed formulation (3.5a)-(3.5d): Find  $(u_h^m, \underline{\underline{\mathbf{p}}}_h^m) \in V_h \times \underline{\underline{\mathbf{M}}}_h$  such that for all

$(v_h, \underline{\mathbf{q}}_h) \in V_h \times \underline{\mathbf{M}}_h$  it holds

(3.10a)

$$\begin{aligned} & \sum_{K \in \mathcal{T}_h} \int_K \underline{\mathbf{p}}_h^m : \underline{\mathbf{q}}_h \, dx + \sum_{K \in \mathcal{T}_h} \int_K \nabla u_h^m \cdot \nabla \cdot (\omega(\nabla u_h^m)^{-1/4} \underline{\mathbf{q}}_h) \, dx - \\ & \sum_{K \in \mathcal{T}_h} \int_{\partial K} \omega(\nabla u_h^m)^{-1/4} \nabla u_h^m \cdot \underline{\mathbf{q}}_h \mathbf{n}_{\partial K} \, ds = 0, \end{aligned}$$

(3.10b)

$$\begin{aligned} & \sum_{K \in \mathcal{T}_h} \int_K u_h^m v_h \, dx + \tau_m \beta \delta^2 \left( \sum_{K \in \mathcal{T}_h} \int_K \underline{\mathbf{p}}_h^m : \underline{\mathbf{A}}_2(u_h^m) D^2 v_h \, dx - \right. \\ & \left. \sum_{K \in \mathcal{T}_h} \int_{\partial K} \underline{\mathbf{A}}_2(u_h^m) \underline{\mathbf{p}}_h^m \mathbf{n}_{\partial K} \cdot \nabla v_h \, ds + \sum_{K \in \mathcal{T}_h} \int_{\partial K} \mathbf{n}_{\partial K} \cdot \nabla \cdot \underline{\mathbf{A}}_2(u_h^m) \underline{\mathbf{p}}_h^m v_h \, ds \right) = \\ & \sum_{K \in \mathcal{T}_h} \int_K u_h^{m-1} v_h \, dx. \end{aligned}$$

A general C<sup>0</sup>DG approximation of (2.1b),(2.1b) is based on the mixed formulation (3.10a),(3.10b) and characterized by numerical flux functions  $\hat{\underline{\mathbf{u}}}_{\partial K}^m$ ,  $\hat{\underline{\mathbf{p}}}_{\partial K}^m$ , and  $\hat{\underline{\mathbf{s}}}_{\partial K}^m$  that are single-valued on  $E \in \mathcal{E}_h(\Omega)$ , i.e.,  $\hat{\underline{\mathbf{u}}}_{\partial K}^m|_{E_+} = \hat{\underline{\mathbf{u}}}_{\partial K}^m|_{E_-}$ ,  $\hat{\underline{\mathbf{p}}}_{\partial K}^m|_{E_+} = \hat{\underline{\mathbf{p}}}_{\partial K}^m|_{E_-}$ , and  $\hat{\underline{\mathbf{s}}}_{\partial K}^m|_{E_+} = \hat{\underline{\mathbf{s}}}_{\partial K}^m|_{E_-}$ . We replace  $\omega(\nabla u_h^m)^{-1/4} \nabla u_h^m \cdot \underline{\mathbf{q}}_h \mathbf{n}_{\partial K}$  in (3.10a) by  $\hat{\underline{\mathbf{u}}}_{\partial K}^m \cdot \underline{\mathbf{q}}_h \mathbf{n}_{\partial K}$  and  $\underline{\mathbf{A}}_2(u_h^m) \underline{\mathbf{p}}_h^m \mathbf{n}_{\partial K} \cdot \nabla v_h = \underline{\mathbf{A}}_2(u_h^m) D^2(u_h^m) \mathbf{n}_{\partial K} \cdot \omega(\nabla u_h^m)^{-1/4} \nabla v_h$  as well as  $\mathbf{n}_{\partial K} \cdot \nabla \cdot \underline{\mathbf{A}}_2(u_h^m) \underline{\mathbf{p}}_h^m v_h$  in (3.10b) by  $\hat{\underline{\mathbf{p}}}_{\partial K}^m \cdot \omega(\nabla u_h^m)^{-1/4} \nabla v_h$  and  $\mathbf{n}_{\partial K} \cdot \hat{\underline{\mathbf{s}}}_{\partial K}^m v_h$ . In view of (3.5d) we choose  $\hat{\underline{\mathbf{s}}}_{\partial K}^m|_E = \mathbf{n}_E \cdot \nabla \cdot \underline{\mathbf{A}}_2(u_h^m) \underline{\mathbf{p}}_h^m = 0$ ,  $E \in \mathcal{E}_h(\Gamma)$ . Then, no matter how we choose  $\hat{\underline{\mathbf{s}}}_{\partial K}^m|_E$  on  $E \in \mathcal{E}_h(\Omega)$ , due to  $[\hat{\underline{\mathbf{s}}}_{\partial K}^m]_E = 0$ ,  $E \in \mathcal{E}_h(\Omega)$ , and  $v_h \in C^0(\bar{\Omega})$  we have

$$(3.11) \quad \sum_{K \in \mathcal{T}_h} \int_{\partial K} \mathbf{n}_{\partial K} \cdot \hat{\underline{\mathbf{s}}}_{\partial K}^m v_h \, ds = \sum_{E \in \mathcal{E}_h(\Omega)} \mathbf{n}_E \cdot [\hat{\underline{\mathbf{s}}}_{\partial K}^m]_E v_h \, ds = 0.$$

Consequently, observing (3.11), in a general C<sup>0</sup>DG approximation, we are looking for a pair  $(u_h^m, \underline{\mathbf{p}}_h^m) \in V_h \times \underline{\mathbf{M}}_h$  such that for all  $(v_h, \underline{\mathbf{q}}_h) \in V_h \times \underline{\mathbf{M}}_h$  it holds

$$(3.12a) \quad \begin{aligned} & \sum_{K \in \mathcal{T}_h} \int_K \underline{\mathbf{p}}_h^m : \underline{\mathbf{q}}_h \, dx + \sum_{K \in \mathcal{T}_h} \int_K \nabla u_h^m \cdot \nabla \cdot (\omega(\nabla u_h^m)^{-1/4} \underline{\mathbf{q}}_h) \, dx - \\ & \sum_{K \in \mathcal{T}_h} \int_{\partial K} \hat{\underline{\mathbf{u}}}_{\partial K}^m \cdot \underline{\mathbf{q}}_h \mathbf{n}_{\partial K} \, ds = 0, \end{aligned}$$

$$(3.12b) \quad \begin{aligned} & \sum_{K \in \mathcal{T}_h} \int_K u_h^m v_h \, dx + \tau_m \beta \delta^2 \left( \sum_{K \in \mathcal{T}_h} \int_K \underline{\mathbf{p}}_h^m : \underline{\mathbf{A}}_2(u_h^m) D^2 v_h \, dx - \right. \\ & \left. \sum_{K \in \mathcal{T}_h} \int_{\partial K} \hat{\underline{\mathbf{p}}}_{\partial K}^m \cdot (\omega(\nabla u_h^m)^{-1/4} \nabla v_h) \, ds \right) = \sum_{K \in \mathcal{T}_h} \int_K u_h^{m-1} v_h \, dx. \end{aligned}$$

In particular, for the  $C^0$ IPDG approximation the numerical flux functions  $\hat{\mathbf{u}}_{\partial K}^m$  and  $\hat{\mathbf{p}}_{\partial K}^m$  are given by

$$(3.13a) \quad \hat{\mathbf{u}}_{\partial K}^m|_E := \begin{cases} \{\omega(\nabla u_h^m)^{-1/4} \nabla u_h^m\}_E, & E \in \mathcal{E}_h(\Omega) \\ \mathbf{0}, & E \in \mathcal{E}_h(\Gamma) \end{cases},$$

$$(3.13b) \quad \hat{\mathbf{p}}_{\partial K}^m|_E := \{\underline{\mathbf{A}}_2(u_h^m) D^2 u_h^m\}_E \mathbf{n}_E - \alpha h_E^{-1} [\omega(\nabla u_h^m)^{-1/4} \nabla u_h^m]_E, \quad E \in \mathcal{E}_h,$$

where  $\alpha > 0$  is a penalty parameter.

**Theorem 3.1.** *The particular choice (3.13a),(3.13b) of the numerical flux functions allows to eliminate the dual variable  $\underline{\mathbf{p}}_h^m$  from the system (3.12a),(3.12b). We thus obtain the  $C^0$ IPDG approximation: Find  $u_h^m \in V_h$  such that for all  $v_h \in V_h$  it holds*

$$(3.14) \quad (u_h^m, v_h)_{0,\Omega} + \tau_m \beta \delta^2 a_h^{IP}(u_h^m, v_h; u_h^m) = (u_h^{m-1}, v_h)_{0,\Omega},$$

where for  $z_h \in V_h$  the mesh-dependent  $C^0$ IPDG form  $a_h^{IP}(\cdot, \cdot; z_h) : V_h \times V_h$  is given by

$$(3.15) \quad a_h^{IP}(u_h, v_h; z_h) := \sum_{K \in \mathcal{T}_h} (\underline{\mathbf{A}}_1(z_h) D^2 u_h, D^2 v_h)_{0,K} - \sum_{E \in \mathcal{E}_h} (\mathbf{n}_E \cdot \{\underline{\mathbf{A}}_2(z_h) D^2 u_h\}_E \mathbf{n}_E, \mathbf{n}_E \cdot [\omega(\nabla z_h)^{-1/4} \nabla v_h]_E)_{0,E} - \sum_{E \in \mathcal{E}_h} (\mathbf{n}_E \cdot \{\underline{\mathbf{A}}_2(z_h) D^2 v_h\}_E \mathbf{n}_E, \mathbf{n}_E \cdot [\omega(\nabla z_h)^{-1/4} \nabla u_h]_E)_{0,E} + \alpha \sum_{E \in \mathcal{E}_h} h_E^{-1} (\mathbf{n}_E \cdot [\omega(\nabla z_h)^{-1/4} \nabla u_h]_E, \mathbf{n}_E \cdot [\omega(\nabla z_h)^{-1/4} \nabla v_h]_E)_{0,E}.$$

*Proof.* If we choose  $\underline{\mathbf{q}}_h = \underline{\mathbf{A}}_2(u_h^m) D^2 v_h$  in (3.12a) and use (3.13a), we obtain

$$(3.16) \quad \sum_{K \in \mathcal{T}_h} \int_K \underline{\mathbf{p}}_h^m : \underline{\mathbf{A}}_2(u_h^m) D^2 v_h \, dx + \sum_{K \in \mathcal{T}_h} \int_K \nabla u_h^m \cdot \nabla \cdot (\omega(\nabla u_h^m)^{-1/4} \underline{\mathbf{A}}_2(u_h^m) D^2 v_h) \, dx - \sum_{E \in \mathcal{E}_h(\Omega)} \int_E \{\omega(\nabla u_h^m)^{-1/4} \nabla u_h^m\}_E \cdot [\underline{\mathbf{A}}_2(u_h^m) D^2 v_h]_E \mathbf{n}_E \, ds = 0.$$

For the second term on the left-hand side of (3.16), applying Green's formula elementwise and observing (2.14),(2.17) yields

$$(3.17) \quad \sum_{K \in \mathcal{T}_h} \int_K \nabla u_h^m \cdot \nabla \cdot (\omega(\nabla u_h^m)^{-1/4} \underline{\mathbf{A}}_2(u_h^m) D^2 v_h) \, dx = - \sum_{K \in \mathcal{T}_h} \int_K D^2 u_h^m : \underline{\mathbf{A}}_1(u_h^m) D^2 v_h \, dx + \sum_{K \in \mathcal{T}_h} \int_{\partial K} \omega(\nabla u_h^m)^{-1/4} \nabla u_h^m \cdot \underline{\mathbf{A}}_2(u_h^m) D^2 v_h \mathbf{n}_{\partial K} \, ds.$$

Now, taking advantage of

$$(3.18) \quad \sum_{K \in \mathcal{T}_h} \int_{\partial K} \underline{\mathbf{p}} \cdot \underline{\mathbf{q}} \mathbf{n}_{\partial K} \, ds = \sum_{E \in \mathcal{E}_h} \int_E [\underline{\mathbf{p}}]_E \cdot \{\underline{\mathbf{q}}\}_E \mathbf{n}_E \, ds + \sum_{E \in \mathcal{E}_h(\Omega)} \int_E \{\underline{\mathbf{p}}\}_E \cdot [\underline{\mathbf{q}}]_E \mathbf{n}_E \, ds$$

with  $\underline{\mathbf{p}} = \omega(\nabla u_h^m)^{-1/4} \nabla u_h^m$  and  $\underline{\mathbf{q}} = \underline{\mathbf{A}}_2(u_h^m) D^2 v_h$ , we get

$$(3.19) \quad \sum_{K \in \mathcal{T}_h} \int_{\partial K} \omega(\nabla u_h^m)^{-1/4} \nabla u_h^m \cdot \underline{\mathbf{A}}_2(u_h^m) D^2 v_h \mathbf{n}_{\partial K} \, ds = \sum_{E \in \mathcal{E}_h} \int_E [\omega(\nabla u_h^m)^{-1/4} \nabla u_h^m]_E \cdot \{\underline{\mathbf{A}}_2(u_h^m) D^2 v_h\}_E \mathbf{n}_E \, ds + \sum_{E \in \mathcal{E}_h(\Omega)} \int_E \{\omega(\nabla u_h^m)^{-1/4} \nabla u_h^m\}_E \cdot [\underline{\mathbf{A}}_2(u_h^m) D^2 v_h]_E \mathbf{n}_E \, ds.$$

Using (3.17) and (3.19) in (3.16) it follows that

$$(3.20) \quad \sum_{K \in \mathcal{T}_h} \int_K \underline{\mathbf{p}}_h^m : \underline{\mathbf{A}}_2(u_h^m) D^2 v_h \, dx = \sum_{K \in \mathcal{T}_h} \int_K D^2 u_h^m : \underline{\mathbf{A}}_1(u_h^m) D^2 v_h \, dx - \sum_{E \in \mathcal{E}_h} \int_E [\omega(\nabla u_h^m)^{-1/4} \nabla u_h^m]_E \cdot \{\underline{\mathbf{A}}_2(u_h^m) D^2 v_h\}_E \mathbf{n}_E \, ds.$$

On the other hand, inserting (3.13b) into (3.12b) and applying again (3.18), we obtain

$$(3.21) \quad \sum_{K \in \mathcal{T}_h} \int_K u_h^m v_h \, dx + \tau_m \beta \delta^2 \left( \sum_{K \in \mathcal{T}_h} \int_K \underline{\mathbf{p}}_h^m : \underline{\mathbf{A}}_2(u_h^m) D^2 v_h \, dx - \sum_{K \in \mathcal{T}_h} \int_{\partial K} \hat{\underline{\mathbf{p}}}_{\partial K}^m \cdot \nabla v_h \, ds \right) = \sum_{K \in \mathcal{T}_h} \int_K u_h^m v_h \, dx + \tau_m \beta \delta^2 \left( \sum_{K \in \mathcal{T}_h} \int_K \underline{\mathbf{p}}_h^m : \underline{\mathbf{A}}_2(u_h^m) D^2 v_h \, dx - \sum_{E \in \mathcal{E}_h} \int_E \{\underline{\mathbf{A}}_2(u_h^m) D^2 u_h^m\}_E \mathbf{n}_E \cdot [\omega(\nabla u_h^m)^{-1/4} \nabla v_h]_E \, ds + \alpha \sum_{E \in \mathcal{E}_h} h_E^{-1} \int_E [\omega(\nabla u_h^m)^{-1/4} \nabla u_h^m]_E \cdot [\omega(\nabla u_h^m)^{-1/4} \nabla v_h]_E \, ds \right) = \sum_{K \in \mathcal{T}_h} \int_K u_h^{m-1} v_h \, dx.$$

The assertion follows from using (3.20) in (3.21).  $\square$

**Remark 3.1.** We note that the  $C^0$ IPDG approximation (3.14) can be derived from the boundary value problem (2.1a),(2.1b) (cf., e.g., [7] for a fourth order boundary value problem related to the biharmonic problem). However, we have chosen the approach via the mixed formulation, since the  $C^0$ DG approximation (3.10a),(3.10b) is more general in so far as another choice of the numerical flux functions than (3.13a),(3.13b) may lead to a different  $C^0$ DG approach as, for instance, a  $C^0$  Local Discontinuous Galerkin ( $C^0$ LDG) method.

#### 4. A PREDICTOR CORRECTOR CONTINUATION STRATEGY FOR THE NUMERICAL SOLUTION OF THE $C^0$ IPDG APPROXIMATION

The solution  $u(x, t)$ ,  $(x, t) \in Q$ , of the fourth order total variation flow problem (1.2) is characterized by

- the formation of facets around local extrema of the initial data with steep gradients at the interfaces,
- a finite extinction time  $t_{ext} > 0$ , i.e.,  $u(x, t) = 0$ ,  $x \in \Omega$ , for  $t \geq t_{ext}$ .

The same behavior can be expected from the solution of the  $C^0$ IPDG approximation (3.14). In particular, the appropriate choice of the time step is a crucial issue when solving the nonlinear system resulting from (3.14). Therefore, it is more advantageous to work with a variable time step  $\tau_m = t_m - t_{m-1}$ ,  $1 \leq m \leq M$ , instead of a uniform time step  $\Delta t = T/M$ ,  $M \in \mathbb{N}$  and to choose  $\tau_m$  such that convergence of a Newton-type method is guaranteed. This can be achieved by viewing (3.14) as a parameter dependent nonlinear system with the time as the parameter and to apply a predictor corrector continuation strategy featuring an adaptive choice of the time step sizes  $\tau_m$  (cf., e.g., [10, 16]).

We assume  $V_h = \text{span}\{\varphi_1, \dots, \varphi_{N_h}\}$ ,  $N_h \in \mathbb{N}$ , such that

$$u_h^m = \sum_{j=1}^{N_h} u_j^m \varphi_j.$$

Setting  $\mathbf{u}^m := (u_1^m, \dots, u_{N_h}^m)^T$ , the algebraic formulation of (3.14) leads to the nonlinear system

$$(4.1) \quad \mathbf{F}(\mathbf{u}^m, t_m) = \mathbf{0},$$

where the components  $\mathbf{F}_i$ ,  $1 \leq i \leq N_h$ , are given by

$$\begin{aligned} \mathbf{F}_i(\mathbf{u}^m, t_m) &= \sum_{j=1}^{N_h} u_j^m (\varphi_j, \varphi_i)_{0,\Omega} + \\ &\quad \tau_m \beta \delta^2 a_h^{DG} \left( \sum_{j=1}^{N_h} u_j^m \varphi_j, \varphi_i; \sum_{j=1}^{N_h} u_j^m \varphi_j \right) - \sum_{j=1}^{N_h} u_j^{m-1} (\varphi_j, \varphi_i)_{0,\Omega}. \end{aligned}$$

Given  $\mathbf{u}^{m-1}$ , the time step size  $\tau_{m-1,0} = \tau_{m-1}$ , and setting  $k = 0$ , where  $k$  is a counter for the predictor corrector steps, the predictor step for (4.1) consists of constant continuation leading to the initial guess

$$(4.2) \quad \mathbf{u}^{(m,k)} = \mathbf{u}^{m-1}, \quad t_m = t_{m-1} + \tau_{m-1,k}.$$

Setting  $\nu = 0$  and  $\mathbf{u}^{(m,k,\nu_1)} = \mathbf{u}^{(m,k)}$ , for  $\nu \leq \nu_{max}$ , where  $\nu_{max} > 0$  is a pre-specified maximal number, the Newton iteration

$$(4.3) \quad \mathbf{F}'(\mathbf{u}^{(m,k,\nu)}, t_m) \Delta \mathbf{u}^{(m,k,\nu)} = -\mathbf{F}(\mathbf{u}^{(m,k,\nu)}, t_m),$$

serves as a corrector whose convergence is monitored by the contraction factor

$$(4.4) \quad \Lambda^{(m,k,\nu)} = \frac{\|\overline{\Delta \mathbf{u}^{(m,k,\nu)}}\|}{\|\Delta \mathbf{u}^{(m,k,\nu)}\|},$$

where  $\overline{\Delta \mathbf{u}^{(m,k,\nu)}}$  is the solution of the auxiliary Newton step

$$(4.5) \quad \mathbf{F}'(\mathbf{u}^{(m,k,\nu)}, t_m) \overline{\Delta \mathbf{u}^{(m,k,\nu)}} = -\mathbf{F}(\mathbf{u}^{(m,k,\nu+1)}, t_m).$$

If the contraction factor satisfies

$$(4.6) \quad \Lambda^{(m,k,\nu)} < \frac{1}{2},$$

we set  $\nu = \nu + 1$ . If  $\nu > \nu_{max}$ , both the Newton iteration and the predictor corrector continuation strategy are terminated indicating non-convergence. Otherwise, we continue the Newton iteration (4.3). If (4.6) does not hold true, we set  $k = k + 1$  and the time step is reduced according to

$$(4.7) \quad \tau_{m,k} = \max\left(\frac{\sqrt{2} - 1}{\sqrt{4\Lambda^{(m,\nu)} + 1} - 1} \tau_{m,k-1}, \tau_{min}\right),$$

where  $\tau_{min} > 0$  is some pre-specified minimal time step. If  $\tau_{m,k} \geq \tau_{min}$ , we go back to the prediction step (4.2). Otherwise, the predictor corrector strategy is stopped indicating non-convergence. The Newton iteration is terminated successfully, if for some  $\nu^* > 0$  the relative error of two subsequent Newton iterates satisfies

$$(4.8) \quad \frac{\|\mathbf{u}^{(m,k,\nu^*)} - \mathbf{u}^{(m,k,\nu^*-1)}\|}{\|\mathbf{u}^{(m,k,\nu^*)}\|} < \varepsilon$$

for some pre-specified accuracy  $\varepsilon > 0$ . In this case, we set

$$(4.9) \quad \mathbf{u}^m = \mathbf{u}^{(m,k,\nu_1^*)}$$

and predict a new time step according to

$$(4.10) \quad \tau_m = \min\left(\frac{(\sqrt{2} - 1) \|\Delta \mathbf{u}^{(m,k,0)}\|}{2\Lambda^{(m,k,0)} \|\mathbf{u}^{(m,k,0)} - \mathbf{u}^m\|}, \text{amp}\right) \tau_{m,k},$$

where  $\text{amp} > 0$  is a pre-specified amplification factor for the time step sizes. We set  $m = m + 1$  and begin new predictor corrector iterations for the time interval  $[t_m, t_{m+1}]$ .

The choice of the contraction factor (4.6), the choice of the reduced time step (4.7), and the choice of the enlarged time step (4.10) are motivated by the affine covariant convergence theory of Newton's method (cf., e.g., [10, 16]).

## 5. NUMERICAL RESULTS

We have implemented the C<sup>0</sup>IPDG method of section 3 along with the predictor corrector continuation strategy of section 5 for two examples. In both cases, we have chosen  $\Omega = (0, 1)^2$ ,  $\beta = 1.0 \cdot 10^{-7}$ , polynomial degree  $k = 2$  and penalization parameter  $\alpha = 200.0$  in the C<sup>0</sup>IPDG method, and  $\nu_{max} = 50$ ,  $\varepsilon = 1.0 \cdot 10^{-3}$ , and  $\tau_{min} = 1.0 \cdot 10^{-8}$  for the predictor corrector continuation strategy.

**Example 1:** The first example is the same as in [22], where the initial data  $u^0$  has been chosen according to

$$u^0(x_1, x_2) = x_1(x_1 - 1)x_2(x_2 - 1) - \frac{1}{36}.$$

The  $C^0$ IPDG approximation  $u_h^m$  has been computed for various regularization parameters  $\delta$  and finite element mesh sizes  $h$ .

For  $\delta = 2.5 \cdot 10^{-4}$  and  $h = 1/10$ , Figure 1 displays the initial data  $u_h^0$  at time  $t = 0.0$  (top left), and the computed solutions at times  $t = 4.6 \cdot 10^{-6}$  (top right),  $t = 2.6 \cdot 10^{-3}$  (bottom left), and  $t = 1.2 \cdot 10^{-2}$  (bottom right). We see that the solution develops facets around local extrema of the initial data with a narrow interface featuring steep gradients in between. The extinction time, i.e., the time when the initial profile gets completely flat, is  $t_{ext} = 1.1 \cdot 10^{-2}$ .

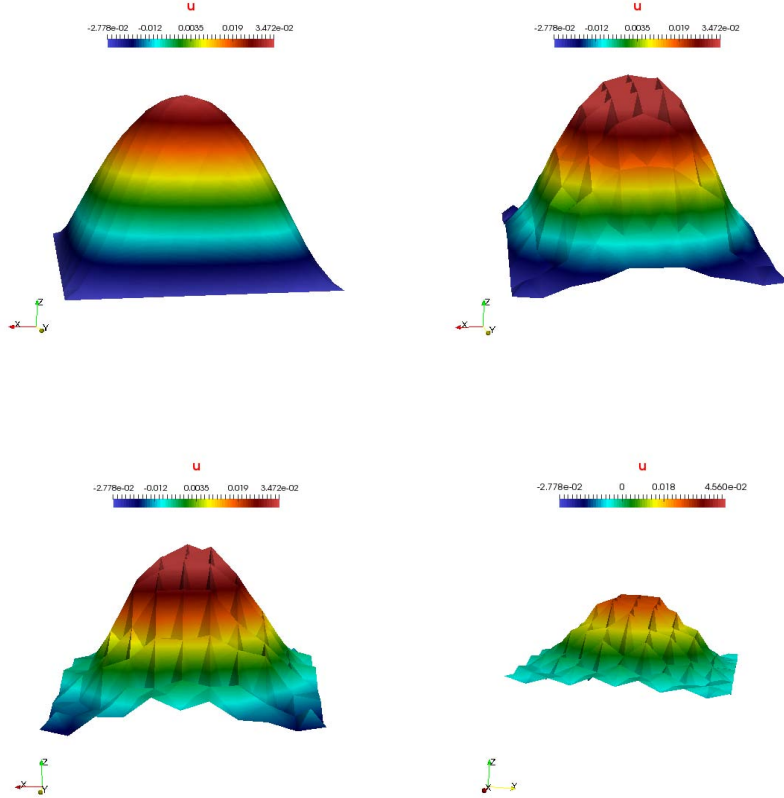


FIGURE 1. Example 1: Computed solution for  $h = 1/10$  and  $\delta = 2.5 \cdot 10^{-4}$  at initial time  $t = 0$  sec (top left), at time  $t = 4.6 \cdot 10^{-5}$  sec (top right), at time  $t = 2.6 \cdot 10^{-3}$  sec, and at time  $t = 1.2 \cdot 10^{-2}$  sec (bottom right).

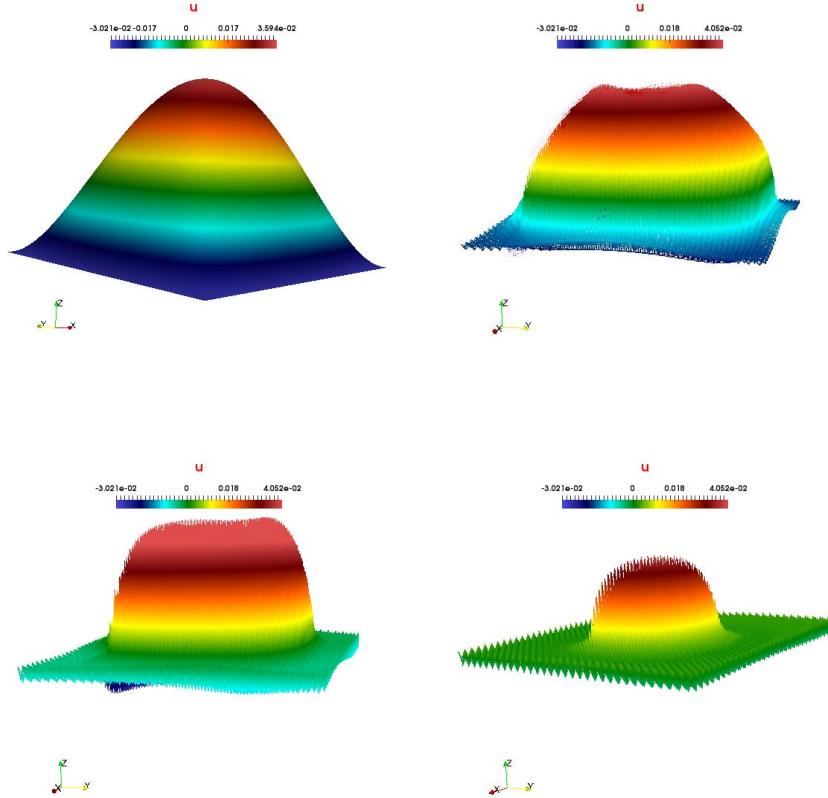


FIGURE 2. Example 1: Computed solution for  $h = 1/64$  and  $\delta = 7.5 \cdot 10^{-3}$  at initial time  $t = 0$  sec (top left), at time  $t = 6.9 \cdot 10^{-7}$  sec (top right), at time  $t = 9.5 \cdot 10^{-5}$  sec, and at time  $t = 1.3 \cdot 10^{-3}$  sec (bottom right).

For  $\delta = 7.5 \cdot 10^{-3}$ , and  $h = 1/64$ , Figure 2 shows the same behavior of the solution. However, due to the significantly smaller mesh size  $h$  the interface between the upper and lower facets is much better resolved. In this case, the extinction time turned out to be  $t_{ext} = 2.2 \cdot 10^{-2}$ .

The performance of the predictor corrector continuation strategy for  $h = 1/10$  and  $\delta = 2.5 \cdot 10^{-4}$  is shown in Figure 3 where the adaptive choice of the time steps  $\tau_m$  is shown as a function of the iterations. We see that the time step sizes are gradually increasing in a step-like way where the individual steps correspond to the formation of the interface between the upper and the lower facets.

Figure 4 shows the corresponding results for the predictor corrector continuation strategy in case  $h = 1/64$  and  $\delta = 7.5 \cdot 10^{-3}$ . The convergence is expected to become a tougher issue for smaller mesh width  $h$  which is reflected by Figure 4.

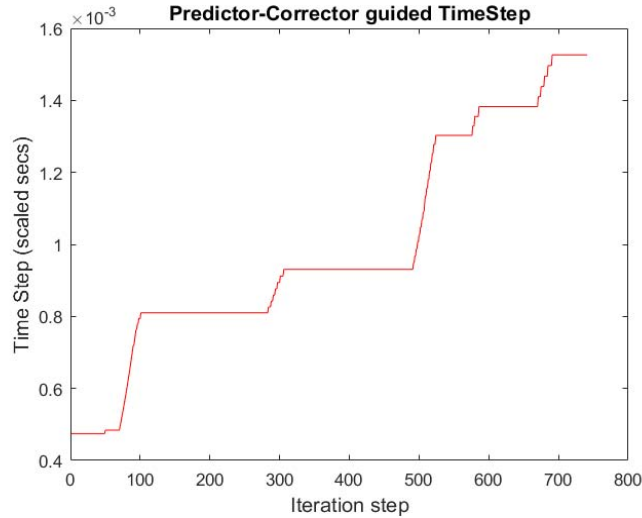


FIGURE 3. Example 1: Performance of the predictor corrector continuation strategy for  $h = 1/10$  and  $\delta = 2.5 \cdot 10^{-4}$ . Adaptive choice of time steps  $\tau_m$ .

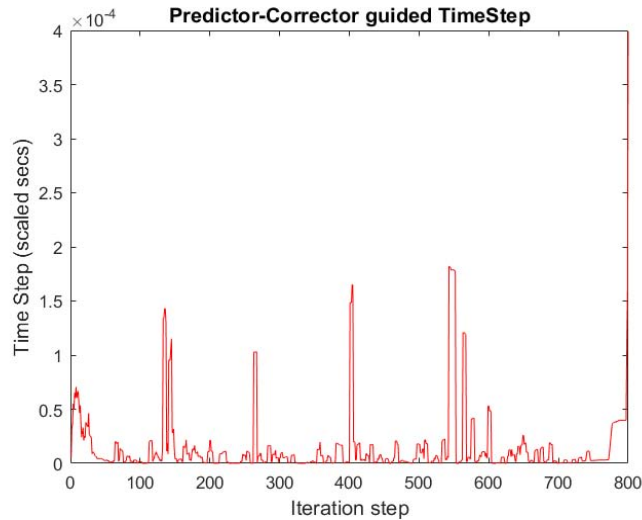


FIGURE 4. Example 1: Performance of the predictor corrector continuation strategy for  $h = 1/64$  and  $\delta = 7.5 \cdot 10^{-3}$ . Adaptive choice of time steps  $\tau_m$ .

As far as the convergence of the  $C^0$ IPDG approximations  $u_h^m$  to the solution  $u^m$ ,  $m \geq 1$ , of (2.1) is concerned, we have computed an experimental convergence rate, since the exact solutions  $u^m$  are not explicitly known. The experimental

convergence rate is given by

$$(5.1) \quad \text{err}(t_m) := \log_2 \frac{\| \|u_h^m - u_{2h}^m\| \|}{\| \|u_{h/2}^m - u_h^m\| \|},$$

where  $\| \| \cdot \| \|$  stands for the norm

$$(5.2) \quad \| \|z_h^m\| \| := \left( \|z_h^m\|_{0,\Omega}^2 + \sum_{\ell=1}^m \tau_\ell \|z_h^\ell\|_{2,h/2,\Omega}^2 \right)^{1/2}.$$

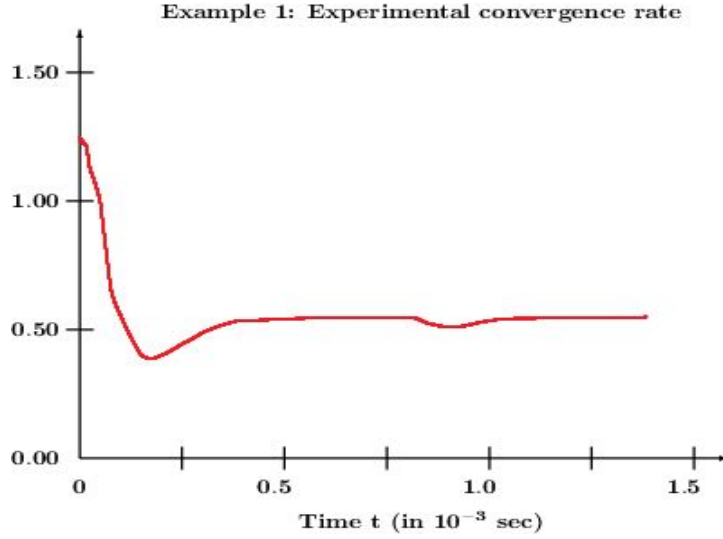


FIGURE 5. Example 1: Experimental convergence rate  $\text{err}(t_m)$  for  $h = 1/64$ .

Figure 5 displays the experimental convergence rate as a function of time for  $h = 1/64$ . Taking into account that the initial data is smooth, at the very beginning the rate drops significantly due to the formation of facets with sharp interfaces between the upper and the lower facet. Afterwards it stabilizes around 0.5.

Forthcoming work will be devoted to provide an a priori error estimate in the  $\| \| \cdot \| \|$ -norm.

**Example 2:** The initial profile  $u^0$  has been chosen according to

$$u^0(x_1, x_2) = \begin{cases} x_1(\frac{1}{2} - x_1)(1 - x_1)x_2(\frac{1}{2} - x_2)(1 - x_2) - \frac{1}{32}, & 0 \leq x_1 < \frac{1}{2}, 0 \leq x_2 < \frac{1}{2} \\ x_1(x_1 - \frac{1}{2})(1 - x_1)x_2(\frac{1}{2} - x_2)(1 - x_2) - \frac{1}{32}, & \frac{1}{2} \leq x_1 \leq 1, 0 \leq x_2 < \frac{1}{2} \\ x_1(\frac{1}{2} - x_1)(1 - x_1)x_2(x_2 - \frac{1}{2})(1 - x_2) - \frac{1}{32}, & 0 \leq x_1 < \frac{1}{2}, \frac{1}{2} \leq x_2 \leq 1 \\ x_1(x_1 - \frac{1}{2})(1 - x_1)x_2(x_2 - \frac{1}{2})(1 - x_2) - \frac{1}{32}, & \frac{1}{2} \leq x_1 \leq 1, \frac{1}{2} \leq x_2 \leq 1 \end{cases}.$$

For  $\delta = 4.5 \cdot 10^{-3}$  and  $h = 1/128$ , Figure 6 shows the route along which the initial profile becomes completely flat. We observe the development of four upper facets around the four maxima of the initial data and lower facets around the minima. Due to the small mesh size  $h$ , the formation of narrow interfaces with steep gradients between the upper and lower facets happens quickly. The extinction time is  $t_{ext} = 1.2 \cdot 10^{-2}$ .

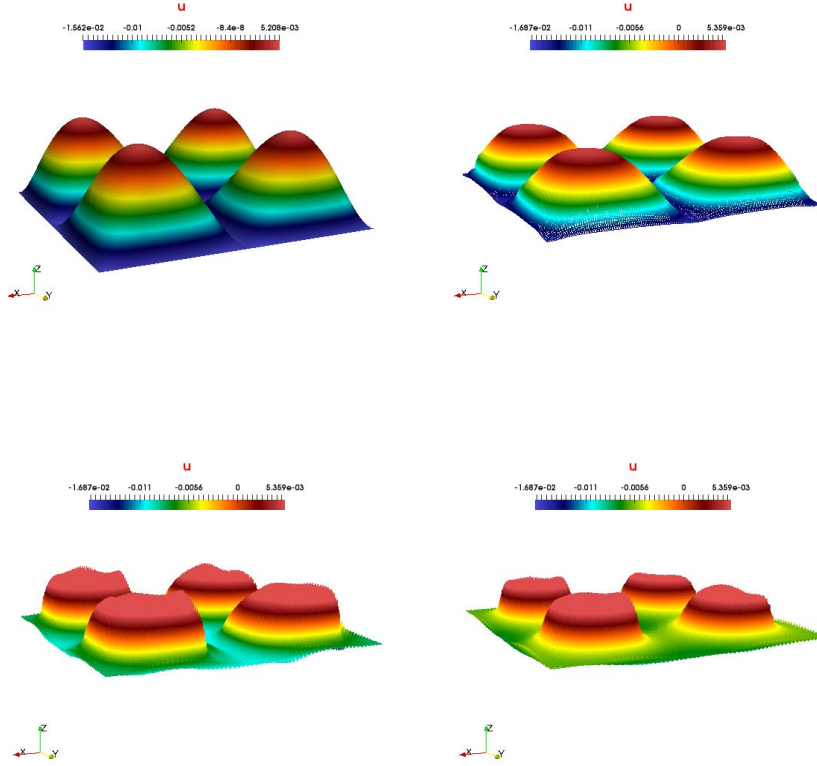


FIGURE 6. Example 2: Computed solution for  $h = 1/128$  and  $\delta = 4.5 \cdot 10^{-3}$  at initial time  $t = 0$  sec (top left), at time  $t = 3.4 \cdot 10^{-5}$  sec (top right), at time  $t = 9.7 \cdot 10^{-3}$  sec (bottom left), and at time  $t = 7.1 \cdot 10^{-2}$  sec (bottom right).

Figure 7 displays the adaptive choice of the time steps. We see a similar behavior as in Example 1 for  $h = 1/64$  and  $\delta = 7.5 \cdot 10^{-3}$ .

## 6. CONCLUSION

We have derived a  $C^0$ IPDG approximation of an implicitly in time discretized, regularized and scaled fourth order TVF problem describing surface relaxation below the roughening temperature. We have further developed a predictor corrector continuation strategy for the numerical solution of the fully discretized problem featuring an adaptive choice of the time steps. Numerical results have been presented that illustrate the performance of the approach.

The existence and uniqueness of a solution of the  $C^0$ IPDG method will be shown in part II of the paper.

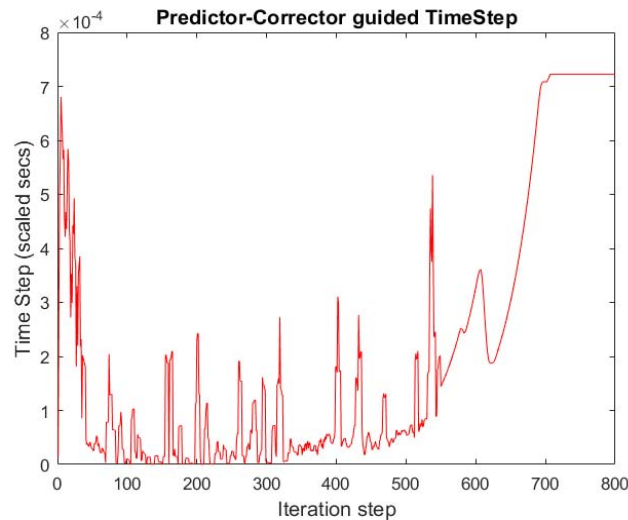


FIGURE 7. Example 2: Performance of the predictor corrector continuation strategy for  $h = 1/128$  and  $\delta = 4.5 \cdot 10^{-3}$ . Adaptive choice of time steps  $\tau_m$ .

#### REFERENCES

- [1] Arnold, D., Brezzi, F., Cockburn, B., and Marini, D., 2002: Unified analysis of discontinuous Galerkin methods for elliptic problems. *SIAM J. Numer. Anal.* **39**, 1749–1779.
- [2] Beirao da Veiga, L., Niiranen, J., and Stenberg, R., 2007: A family of  $C^0$  finite elements for Kirchhoff plates I: Error analysis. *Siam J. Numer. Anal.* **45**, 2047–2071.
- [3] Beirao da Veiga, L., Niiranen, J., and Stenberg, R., 2008: A family of  $C^0$  finite elements for Kirchhoff plates II: Numerical results. *Comput. Meths. Appl. Mech Engrg.* **197**, 1850–1864.
- [4] Braess, D., Hoppe, R.H.W., and Linsenmann, C., 2016: A two-energies principle for the biharmonic equation and an a posteriori error estimator for an interior penalty discontinuous Galerkin approximation. *ESAIM: M2AN*, DOI: <http://dx.doi.org/10.1051/m2an/2016074>.
- [5] S.C. Brenner, S.C., M. Neilan, M., A. Reiser, A., and L.-Y. Sung, L.-Y., 2017: A  $C^0$  interior penalty method for a von Kármán plate. *Numer. Math.* **135**, 803–832.
- [6] Brenner, S.C., Oh, M., Pollock, S., Porwal, K., Schedensack, M., and Sharma, N., 2016: A  $C^0$  interior penalty method for elliptic distributed optimal control problems in three dimensions with pointwise state constraints. In: *Topics in Numerical Partial Differential Equations and Scientific Computing* (S.C. Brenner, ed.), IMA Volumes in Mathematics and Its Applications **160**, 1–22.
- [7] Brenner, S.C. and Sung L.-Y., 2005:  $C^0$  interior penalty methods for fourth order elliptic boundary value problems on polygonal domains. *J. Sci. Comput.*, **22/23**, 83–118.
- [8] Chan, W.L., Ramasubramaniam, A., Shenoy, V.B., and Chason, E., 2004: Relaxation kinetics of nano-ripples on Cu(001) surfaces. *Phys. Rev.* **B 70**, 245403.
- [9] Ciarlet, P.G., 2002: *The Finite Element Method for Elliptic Problems*. SIAM, Philadelphia.
- [10] Deuffhard, P., 2004: *Newton Methods for Nonlinear Problems - Affine Invariance and Adaptive Algorithms*. Springer, Berlin-Heidelberg-New York.
- [11] Engel, G., Garikipati, K., Hughes, T.J.R., Larson, M.G., Mazzei, L., and Taylor, R.L., 2002: Continuous/discontinuous finite element approximations of fourth order elliptic problems in structural and continuum mechanics with applications to thin beams and plates, and strain gradient elasticity. *Comput. Methods Appl. Mech. Engrg.* **191**, 3669–3750.
- [12] Georgoulis, E.H. and Houston, P., 2009: Discontinuous Galerkin methods for the biharmonic problem. *IMA J. Numer. Anal.* **29**, 573–594.

- [13] Giga, M.-H., and Giga, Y., 2010: Very singular diffusion equations: second and fourth order problems. *Jpn. J. Ind. Appl. Math.* **27**, 323–345.
- [14] Giga, Y. and Kohn, R.V., 2011: Scale-invariant extinction time estimates for some singular diffusion equations. *Discrete Contin. Dyn. Syst.* **30**, 509–535.
- [15] Hager, J. and Spohn, H., 1995: Self-similar morphology and dynamics of periodic surface profiles below the roughening transition. *Surface Science* **324**, 365–372.
- [16] Hoppe, R.H.W. and Linsenmann, C., 2012: An adaptive Newton continuation strategy for the fully implicit finite element immersed boundary method. *J. Comp. Phys.* **231**, 4676–4693.
- [17] Hoppe, R.H.W. and Linsenmann, C., 2019:  $C^0$  Interior Penalty Discontinuous Galerkin approximation of a sixth order Cahn-Hilliard equation modeling microemulsification processes. In: *Contributions to Partial Differential Equations and Applications* (B.N. Chetveruskin et al., eds.), Chapter 16, ECCOMAS Series Computational Methods in Applied Sciences. Springer, Berlin-Heidelberg-New York.
- [18] Huang, X. and Huang, J., 2014: A reduced local  $C^0$  discontinuous Galerkin method for Kirchhoff plates. *Numer. Meth. Part. Diff. Equat.* **30**, 1902–1930.
- [19] Kashima, Y., 2004: A subdifferential formulation of fourth order singular diffusion equations. *Adv. Math. Sci. Appl.* **14**, 49–74.
- [20] Kashima, Y., 2004: A variational approach to very singular gradient flow equations. In: *Proceedings of Czech-Japanese Seminar in Applied Mathematics 2004, August 4-7, 2004*, pp. 79–84, Czech Technical University in Prague.
- [21] Kashima, Y., 2012: Characterization of subdifferentials of a singular convex functional in Sobolev spaces of order minus one. *J. Funct. Anal.* **262**, 2833–2860.
- [22] Kohn, R.V. and Versieux, H.M., 2010: Numerical analysis of a steepest-descent PDE model for surface relaxation below the roughening temperature. *SIAM J. Numer. Anal.* **48**, 1781–1800.
- [23] Margetis, D., Aziz, M.J., and Stone, H.A., 2005: Continuum approach to self-similarity and scaling in morphological relaxation of a crystal with a facet. *Physical Review B* **71**, 165432.
- [24] Meyer, Y., 2002: *Oscillating Patterns in Image Processing and Nonlinear Evolution Equations*. Univ. Lecture Ser. 22, AMS, Providence, RI.
- [25] Mozolevski, I. and Süli, E., 2003: A priori error analysis for the hp-version of the discontinuous Galerkin finite element method for the biharmonic equation. *Comput. Methods Appl. Math.* **3**, 1–12.
- [26] Mozolevski, I., Süli, E., and Bösing, P.R., 2007: ; hp-version a priori error analysis of interior penalty discontinuous Galerkin finite element approximations to the biharmonic equation. *J. Sci. Comput.* **30**, 465–491.
- [27] Osher, S., Solé, A., and Vese, L.A., 2003: Image decomposition and restoration using total variation minimization and the  $H^{-1}$  norm. *Multiscale Model. Simul.* **1**, 349–370.
- [28] Ramana Murty, M.V., 2000: ; Morphological stability of nanostructures. *Phys. Rev. B* **62**, 17004-17011.
- [29] Rettori, A. and Villain, J., 1988: ; Flattening of grooves on a crystal surface : a method of investigation of surface roughness. *J. Phys. France* **49**, 257-267.
- [30] Shenoy, V.B., Ramasubramaniam, A., and Freund, L.B., 2003:; A variational approach to nonlinear dynamics of nanoscale surface modulations. *Surf. Sci.* **529**, 365–383.
- [31] Spohn, H., 1993: Surface dynamics below the roughening transition. *J. Phys. I. France* **3**, 69–81.
- [32] Süli, E. and Mozolevski, I., 2007: hp-version interior penalty DGFEMs for the biharmonic equation. *Comput. Methods Appl. Mech. Eng.* **196**, 1851–1863.
- [33] Tartar, L., 2007: *Introduction to Sobolev Spaces and Interpolation Theory*. Springer, Berlin–Heidelberg–New York.
- [34] Vese, L.A. and Osher, S., 2003: Modeling textures with total variation minimization and oscillating patterns in image processing. *J. of Sci. Comput.* **19**, 553–572.
- [35] Vese, L.A. and Osher, S., 2004: Image denoising and decomposition with total variation minimization and oscillatory functions. *J. Math. Imaging Vision* **20**, 7–18.
- [36] Wells, G.N., Kuhl, E., and Garikipati, K., 2006: A discontinuous Galerkin method for the Cahn-Hilliard equation. *J. Comp. Phys.* **218**, 860–877.